

QC
807.5
U6B5
no.14
c.2

Technical Memorandum EDS BOMAP-14



GEOSTROPHIC MOTION FOR THE BOMEX OCEANIC VOLUME

Victor E. Delnore

Center for Experiment Design and Data Analysis
Washington, D.C.
March 1975

noaa

NATIONAL OCEANIC AND
ATMOSPHERIC ADMINISTRATION

Environmental Data
Service

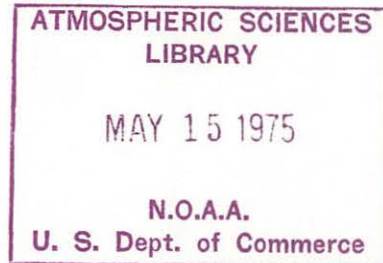
NOAA Technical Memorandum EDS BOMAP-14

OC
807.5
UGB5
70.14
C.2

GESTROPHIC MOTION FOR THE BOMEX OCEANIC VOLUME

Victor E. Delnore

Center for Experiment Design and Data Analysis
Washington, D.C.
March 1975



UNITED STATES
DEPARTMENT OF COMMERCE
Frederick B. Dent, Secretary

NATIONAL OCEANIC AND
ATMOSPHERIC ADMINISTRATION
Robert M. White, Administrator

Environmental Data
Service
Thomas S. Austin, Director



74 5263

CONTENTS

	<u>Page</u>
Abstract	1
1. Introduction	1
2. Relative profiles of geostrophic velocity	2
3. Absolute motion	4
3.1 Method 1: relative profiles of the two main diagonals adjusted by reference to current measurements at the center of the array	6
3.2 Method 2: relative profiles of outer walls each adjusted according to Defant's method for defining the layer of no motion	7
3.3 Method 3: consideration of surface drift calculations . . .	8
3.4 Method 4: layer-by-layer budgets of heat and salt content .	9
4. Property fluxes	9
5. Conclusions	10
Acknowledgements	10
References	11

GEOSTROPHIC MOTION FOR THE BOMEX OCEANIC VOLUME

Victor E. Delnore*

Abstract. The large number of salinity-temperature-depth soundings obtained during part of the 1969 Barbados Oceanographic and Meteorological Experiment (BOMEX) has allowed an analysis of the geostrophic motion east of the Lesser Antilles Arc. Several methods were attempted for determining the motion, and comments are made regarding the applicability of each. The two most successful of these methods yielded absolute geostrophic velocities of several centimeters per second to the northwest and to the southwest. Time series of some of the original data are presented. Because of the large distances between stations, no heat or salinity flux estimates are given.

1. INTRODUCTION

A large number of temperature and salinity profiles from the sea surface to a depth of 1 km were gathered during the field phase of the Barbados Oceanographic and Meteorological Experiment (BOMEX) in 1969. These data were obtained simultaneously over a large oceanic area from five ships at fixed positions. The long, systematically sampled and well-documented series of subsurface measurements from the ships allowed an analysis of the geostrophic motion for the BOMEX water volume.

The circulation of the southwest North Atlantic Ocean had been the subject of several studies (Metcalf, 1968; Ryther, Menzel, and Corwin, 1967) before BOMEX. The makeup and spreading of the waters in this region and the bathymetry affecting their flow have been described by Wüst (1964). More recent studies include one by Warsh, Echternacht, and Garstang (1971) dealing with surface currents, one by Mazeika (1973) on the geostrophic flow from roving-ship data, and a report on the moored BOMEX current meters by Hubertz (1972). Except for Mazeika's study, which shows a high degree of spatial variability in the currents, the flow in this region is generally represented as a persistent (but not stationary) flow to the west-northwest at several centimeters per second.

The field operations during the first three BOMEX observation periods, May 3 to July 2, were designed primarily to measure the exchange rates of heat and water across the air-sea interface (Holland, 1970). Some results of

*This memorandum is based on work done in 1973 when the author, now a postgraduate student at Old Dominion University, was affiliated with the Center for Experiment Design and Data Analysis.

the air-sea interaction program have been reported by Holland (1972), Delnore (1972), and Holland and Rasmusson (1973). In addition to the deployment of weather instruments on ships, aircraft, and balloons, phenomena below the ocean surface were investigated with an array of current meters at various depths and locations and through oceanographic measurements from both the fixed-station and roving ships. Based on these oceanographic measurements, an attempt is made in this paper to deduce the absolute flow from the distribution of mass in the BOMEX water volume. It will be seen, however, that such estimates are, at best, very gross approximations. BOMEX was not designed as an oceanographic-scale experiment, and the station spacing was simply too great to support meaningful water flow calculations.

2. RELATIVE PROFILES OF GEOSTROPHIC VELOCITY

Profiles of salinity and temperature were obtained with Plessey Environmental Systems 9006 and 9040 salinity-temperature-depth (STD) multisensor units lowered from the NOAA ships *Discoverer*, *Oceanographer*, *Mt. Mitchell*, and *Rainier*, and the Coast Guard Cutter *Rockaway*, positioned as shown in figure 1. The square measured 500 km on a side. The two westernmost ships made four soundings per day, and the remaining ships made eight, all spaced approximately equally around the clock (BOMAP Office, 1971).

On each ship the data were recorded as analog frequencies on magnetic tape. The recorded data were later digitized at eight samples per second and then edited and transformed into units of salinity, temperature, and pressure. Fuller discussion of the data processing is contained in BOMEX Period III Upper Ocean Soundings (Delnore and McHugh, 1972). The salinities and temperatures for each corner station for each integer decibar of pressure were averaged over the time interval June 21 through June 30, 1969. (Data from the center station were not sufficiently documented to allow inclusion in an intership analysis.) Time histories of the depths of selected isotherms for June 20 through July 2 are given in figures 2 to 5, and some of the values resulting from the averaging are shown in figure 6. Figure 7 shows the time histories of dynamic depth anomaly (explained below) of certain isobars for one of the stations. Although time averages were used in this analysis, the time histories are presented to allow some appreciation of the regularity of the data. Data are lacking for June 27, which was devoted to maintenance and calibration.

The dynamic depth anomalies at a vertical resolution of 1 decibar were calculated for each of the four corner stations from the time-averaged salinities and temperatures, and the profiles of the differences in dynamic depth anomaly were constructed for each pair of stations from the anomalies at each 10-decibar level.¹ These profiles are given in figure 8, which has two horizontal scales: one for dynamic depth anomaly difference and one for normal component of geostrophic velocity relative to motion at the sea surface. The two scales are related by the lower scale being the product of the upper scale

¹The Coriolis parameter was held constant at its value for the middle latitude of the array, 15°N, so that divergence could be eliminated.

and the Coriolis parameter times the distance between the stations. The interstation distance is greater for the two main diagonals than for the outside boundaries of the BOMEX array; thus the lower scale does not apply to the curves A-E and B-D in figure 8. The method used here for calculating the dynamic depth anomalies and the resulting relative current components is given by Neumann and Pierson (1966) and is outlined below.

When a pressure gradient exists at a given geometric level in a certain area of the ocean, water will flow away from the region of higher pressure. Once the flow is underway, the Coriolis acceleration alters the current's direction. With perfect balance between the pressure and Coriolis forces, the flow will be maintained along the contour lines of pressure. This balance of forces can be represented by equating the Coriolis force to that of the pressure gradient:

$$cf = -\frac{1}{\rho} \frac{\partial p}{\partial n} \quad , \quad (1)$$

where c is the current speed, f is the Coriolis parameter, ρ is water density, and $\partial p/\partial n$ is the pressure gradient. This becomes, for an isobar,

$$c = \frac{-g}{f} \tan\beta \quad , \quad (2)$$

where g is the acceleration of gravity, and β is the geometric slope of the isobar. Only the component of the current normal to the vertical plane joining the two stations can be calculated, and this can be done only in reference to some known current at another pressure level. In spite of the restricted nature of this calculated component, the method is extremely useful for estimating complete vertical profiles of currents relative to an assumed or measured current at some known depth.

In this study, a differential form of (2) was used as a starting point:

$$c_2 - c_1 = \frac{g}{f} (\tan\beta_1 - \tan\beta_2) = \frac{g}{f} \frac{h_A - h_B}{x_{AB}} \quad , \quad (3)$$

where the numerical subscripts denote different isobaric surfaces; the alphabetical subscripts indicate values at stations A and B, respectively; h_A and h_B are the differences in vertical height between the two isobars at station A and station B; and x_{AB} is the horizontal distance between the two stations. Further simplification results through use of the dynamic meter, D , where $D = gh/10 \text{ m}^2 \text{ s}^{-2}$ when h is expressed in geometric meters. The simplification yields:

$$c_2 - c_1 = \frac{-10}{fx_{AB}} \left\{ (D_{2A} - D_{1A}) - (D_{2B} - D_{1B}) \right\} \quad . \quad (4)$$

The quantity ($D_{2A} - D_{1A}$), the difference in dynamic depth (expressed in dynamic meters) between isobars 1 and 2 at station A, can be expressed by

$$D_{2A} - D_{1A} = \int_{p_1}^{p_2} \alpha_A dp, \quad (5)$$

where p is hydrostatic pressure; α is the specific volume of sea water, is a function of salinity, temperature, and pressure, and is given by $\alpha = \alpha_{35,0,p} + \delta$; $\alpha_{35,0,p}$ is the specific volume at 35‰ salinity, 0°C, and pressure p ; and δ is the dynamic volume anomaly, representing departures of α from $\alpha_{35,0,p}$. Since α_A and α_B may differ from each other on the same isobar only through δ , (4) is equivalent to

$$c_2 - c_1 = \frac{10}{f_{x_{AB}}} \left\{ \int_{p_1}^{p_2} \delta_A dp - \int_{p_1}^{p_2} \delta_B dp \right\}. \quad (6)$$

Note that this method yields only differences in velocity components, not the components themselves. The reference velocity, c_1 , still remains to be found. For figure 8, c_1 and p_1 have both been set to zero, giving c_2 in units relative to the velocity component at the sea surface. Thus the profiles in this figure are termed profiles of relative geostrophic velocity component.

3. ABSOLUTE MOTION

Several methods were attempted for establishing the absolute field of motion in the water volume, some of them more applicable than others. In some, the relative geostrophic profiles derived above were used. Others were based on layer-by-layer budgets of heat and salt content, and are discussed below. Vertical motion was assumed to be negligible.

In what follows, the term "BOMEX volume" refers to the prism of water bounded by the sea surface, a roughly horizontal isobaric surface of 1,000-decibar pressure (at a depth of about 995 m), and the four vertical walls that intersect the sea surface along the lines AB, BE, DE, and AD in figure 1. "BOMEX array" denotes the two-dimensional configuration shown as the square ABED in figure 1. "Outer wall" indicates that part of one of the vertical walls that forms one of the boundaries of the BOMEX volume, while "main diagonal" is the portion of a vertical wall through AE or BD within the BOMEX volume. "Stationary" as used here means invariant (or nearly so) with time over the period June 21 through June 30, 1969, the time during which the data for this analysis were obtained.

In ordering values of parameters in the vertical direction, pressure in decibars and depth in meters, being numerically nearly equivalent, are used interchangeably except where a distinction is required. The actual computations were performed in the pressure domain, at a vertical resolution of 1 decibar. Values of temperature in degrees Celsius, salinities in parts per

thousand, and dynamic meters were carried to the third decimal place in all computations. (Note that 1 dynamic meter = $10 \text{ m}^2 \text{ s}^{-2}$.)

Table 1 gives the mean salinity, temperature, and density for each 100-m layer. Each value was obtained by averaging over all four corners and all depths within the appropriate layer. In view of the poor spatial resolution, these values should be regarded only as gross estimates.

Vector diagrams for two moored current-meter arrays, each containing one meter at 1,500 m and another at 2,000 m, have been given by Hubertz (1972), and are reproduced in figure 9. Array I was placed near the center of the line DE (fig. 1). Array II was placed at the center of the BOMEX square and also included a third moored meter at a depth of 300 m. A progressive vector diagram for the current measurements from 300 m given by Mazeika (1973) is reproduced in figure 10.

For the period considered in this study, the two deepest meters at the center of the array showed a nearly stationary current of about 5 cm s^{-1} to the north-northwest (about 342° true), regardless of depth. The apparent currents from Array I, however, were different both from those measured by Array II and also from each other. This suggests two things: (1) that the scale of horizontal dynamic motion is much smaller than the 500-km station spacing of the BOMEX fixed ships, and (2) that there may have been a thick barotropic layer at the center of the BOMEX array. The first of these suggestions is supported by Mazeika's (1973) circulation study based on roving-ship data, in which the dynamic topography of the sea surface is shown to support many shear zones within the BOMEX array.

Table 1.--Mean values of density, salinity, and temperature for each 100-m layer

Layer (m)	ρ (g cm^{-3})	S (‰)	T ($^\circ\text{C}$)
0-100	1.024	35.858	26.926
100-200	1.026	36.771	20.130
200-300	1.027	36.028	15.670
300-400	1.027	35.560	12.898
400-500	1.027	35.280	11.041
500-600	1.027	35.036	9.302
600-700	1.027	34.836	7.696
700-800	1.027	34.652	6.611
800-900	1.027	34.695	5.899
900-1,000	1.027	34.727	5.488

Because the scale of dynamic motion is much less than the sample spacing, it is somewhat futile to attempt to obtain budgets of potential temperature and salinity for the BOMEX volume. Although the net water flux through each outer wall of the volume can be determined (assuming that the geostrophic velocity components can be properly converted from relative to absolute), there are many changes and reversals in trend of salinity, temperature, density, and current along the intersection of any isobar with the outer wall between any two stations in the array. Thus, the flux of the conservative parameters through an outer wall cannot be determined although the net water flux is known. For a budget study, salinities and temperatures spaced no more than 30 nmi along each line would be needed (roughly half the width of the apparent shear zones found by Mazeika), and these would have to be obtained within a time much less than the 1-month period apparently required for typical flows in the BOMEX volume to reverse themselves (figs. 9 and 10). Needless to say, the more closely spaced salinity and temperature measurements would themselves give rise to geostrophic velocity profiles at the finer spatial resolution. That the scale of horizontal variability of dynamic height in the subtropical north Atlantic Ocean is much smaller than the BOMEX station spacing has been further suggested by data from the Mid-Ocean Dynamics Experiment (Scarlet, 1974). These data were obtained at much finer spatial resolution than were the BOMEX data.

In summary, even though the STD data were obtained at a very fine temporal resolution and over a long time period, permitting exceptionally accurate time averaging for the purpose of obtaining net relative geostrophic water transports, the very large spacing between stations compared with the apparent scale of dynamic motion precludes any beneficial use of these data in determining property budgets.

Several methods for estimating the absolute motion in the BOMEX volume are discussed in the sections that follow.

3.1 Method 1: Relative Profiles of the Two Main Diagonals Adjusted by Reference to Current Measurements at the Center of the Array

The relative velocity components normal to the two main diagonals were combined at 10-decibar intervals from the sea surface to 1,000 decibars to form a vector relative to the surface motion and varying with depth. This vector was calculated from time-averaged data for June 21 through June 30, and was assumed to represent the relative net horizontal motion in three dimensions for the interior of the BOMEX volume. This vector was then converted to an absolute vector by extrapolating to 1,500 and 2,000 m so that the extrapolated value approximated the velocity measured by the moored meters at these depths. In other words, the profiles determined by the geostrophic method for the interior of the volume were simply shifted so that their depth-extrapolated values were equal to the values from the meters moored at 1,500 and 2,000 m, and the velocities for all other depths were shifted accordingly to maintain the shapes of the profiles relative with depth. (It is assumed that the currents measured by the deep-moored meters have only geostrophic constituents.)

The hodograph for this vector, now representing an estimate of the absolute large-scale interior motion, is given in figure 11. The second hodograph in that figure will be explained later.

An alternate conversion could have been effected by forcing the 300-m value of the relative vector to agree with the output of the meter at that depth (a nearly stationary value of 6.25 cm s^{-1} to the north-northwest), but it is probable that the match-up with the greater depths is more reliable. The effect of the alternate conversion can be seen by simply moving the entire hodograph, without rotation, so that its 300-m point is coincident with the point marked as representing the 300-m current-meter data (straight dashed line, fig. 11).

Objection may be raised to the validity of single-point current measurements over a great expanse of ocean. Also, there is really no reason to require that the net geostrophic transports calculated across each of the two main diagonals be coincident at the center of the array so as to form a vector. Because of this, it is not clear what physical significance can be properly attributed to this hodograph, except that it may indicate the general trend with depth of the direction and magnitude of the net interior motion.

3.2 Method 2: Relative Profiles of Outer Walls Each Adjusted According to Defant's Method for Defining the Layer of No Motion

According to a 1941 study by Defant (cited in Defant, 1964, p. 710), the vertical gradient in a geostrophic current profile is minimal in the layer that is motionless or nearly so. Application of this principle to the outer-wall profiles shown in figure 8 (solid lines) suggests layers of no motion at the depths indicated by the double-headed arrows alongside three of the profiles in that figure. The profiles with such layers were then shifted along the horizontal axis, and the remaining outer-wall profile was positioned so as to balance the water flux with the other three. (A balanced budget at any depth will force balanced budgets at all depths, since the square in fig. 1 is closed at all depths.) The result of this repositioning is given in figure 12. An apparent level of no motion is seen at about 700 m, but it must be borne in mind that, within the concept of Defant's method, this really represents simply the depth at which the net flux through each of the outer walls is near zero.

This method for estimating the absolute currents in the BOMEX volume is attractive for several reasons. There is no need to assume that point measurements are representative of currents over a large area, no dependence upon empirical formulas relating windspeed and water velocity is needed, and the geostrophic relationship giving layer-by-layer current speed changes is preserved. Further, it does seem plausible that a thick layer with the same speed must have a very low, possibly zero, speed, in accordance with Defant's original arguments.

It must be pointed out, however, that the requirement that a thick layer of zero or near-zero velocity coincident with a layer where the vertical gradient

of dynamic depth anomaly difference is minimal is not compatible with the notion of the steady 5 cm s^{-1} geostrophic current at both 1,500 and 2,000 m in the center of the BOMEX array. Yet it is very unlikely that the velocity between 1,500 and 2,000 m and between 1,000 and 1,500 m is very different from 5 cm s^{-1} , because otherwise the required shears would be very unusual. This is the main inconsistency between application of Defant's method and the use of the data from the deep-current moored meters in estimating the absolute flow, if indeed the currents measured by the meters were substantially geostrophic.

Figure 11 contains, in addition to the one discussed above, a hodograph constructed by combining the fluxes shown in figure 12 so as to form a vector giving the magnitude and direction of absolute motion suggested by the application of Defant's method. The shape of the hodograph is, of course, identical to that of the one previously described, since they are both constructed from the same geostrophic data and differ only by the choice of method in conversion from relative to absolute motion.

3.3 Method 3: Consideration of Surface Drift Calculations

No matter what the profiles of relative or absolute geostrophic current show, there must be a region close to the sea surface whose motion is driven as much by direct wind stress as by the balance of pressure gradient and Coriolis forces. This can be especially true in an area such as the one under consideration, where there is a steady wind of long duration and considerable fetch. If a wind velocity of 15 kn from the east is assumed over the entire BOMEX array, then the sea-surface drift velocity, according to Sverdrup et al. (1942, p. 494), is about 20 cm s^{-1} to the northwest. This agrees roughly with the results of a study by N. Delver (1973, personal communication) of near-station drifting of the five BOMEX ships after their deep-sea moorings had failed in the early part of the experiment and they had to maintain their "fixed" positions by operating in an alternating steaming and drifting mode. His study, based on a tedious renavigation of the ships' reported Omega and dead-reckoning positions, yielded drift vectors for the individual BOMEX ships. When the drifts were spatially interpolated and then broken down into components normal to the lines between the stations shown in figure 1, surface drifts of several centimeters per second to the west and to the north became apparent. These drifts were, of course, the result of the combined effects of wind and current, rather than current alone, since a drifting ship acts both as a sail and as a float.

It is difficult and perhaps of dubious value to match up the geostrophic profiles in figure 8 or 12 with assumed conditions at the surface, especially since the drift estimates obtained by interpolation from the drifts calculated for the corners of the array are probably not indicative of the average drifts. Indeed, in view of the narrow shear zones found by Mazeika (1973) there are probably no meaningful averages for the values of drift across or along each outer wall. Thus no attempt was made to reconcile the surface conditions with the shallow portions of the geostrophic velocity profiles.

3.4 Method 4: Layer-by-Layer Budgets of Heat and Salt Content

Fomin (1964) and Neumann and Pierson (1966) describe a method by K. Hidaka for calculating the absolute velocity fluxes through the boundaries of a volume, which consists of writing and solving, for the configuration in figure 1, equations for the conservation of salt and heat in each of the two major triangular prisms for each layer. Since the horizontal fluxes of mass, salt, and heat into and out of each prism and each layer are forced to balance, vertical motion is denied.

By Hidaka's method, two physical properties (salinity and temperature were the only ones available for this study) must be known for the three vertical boundaries of a triangular prism, and the flux of these properties through one of the boundaries must also be known. In applying this method, the BOMEX volume was bisected into two triangular prisms, ABD and BDE, by the main diagonal, BD (fig. 1), and each of these was then vertically subdivided into 10 equally thick layers. The salinities and heat contents for the vertical boundaries were calculated by simple spatial averaging from the STD profiles, and the water flux through the main diagonal BD was estimated by normalizing the relative geostrophic velocity profile for the line BD to the current meter moored at 300 m. The transports and current profiles obtained varied erratically from layer to layer and were not compatible with generally known ocean conditions. The process was therefore repeated with triangles ABE and ADE, and with the normalized velocity profile for the line AE for the known velocities. Also both processes were repeated with 100 layers rather than 10. No significant departures from the first results were found.

Quite possibly, the BOMEX volume is ill-conditioned for application of Hidaka's method. In particular, in some layers the isohalines and isotherms are so nearly concurrent and level that anomalously high calculated velocities result. The profiles of absolute velocity obtained with this method, even without the instabilities in certain layers, are markedly different from those obtained through use of the geostrophic method for the outer walls. Therefore, it seems that it is quite inconsistent to start with a geostrophic flow on the diagonals and then allow ageostrophic components on the outer walls. This is a fault of the use made in this application of Hidaka's method, not a fault of the method itself. Also, in forming the budget equations for each triangular prism, the salinity and temperature at each depth for each wall were both, by necessity, two-point averages and thus were not really representative of the averages along each 500-km line. Reservations about representing the salinities and temperatures of the outer walls in this manner were given earlier. For these reasons and because of other objections pointed out by Fomin (1964), this method was not pursued further.

4. PROPERTY FLUXES

The two hodographs in figure 11 represent the two most reasonable attempts to determine the absolute flow in the upper 1,000 m of the ocean in the BOMEX area from the STD and current-meter data. As stated earlier, the upper hodograph was constructed by converting the geostrophic profiles of the two main

diagonals from relative to absolute current by normalizing to the measured currents at 1,500 and 2,000 m. The lower one was obtained by shifting the individual geostrophic profiles for the outer walls according to Defant's (1941) method for finding the layer of no motion and then combining the new profiles into vectors. Neither one of these methods appears to be more reliable than the other, given the constraints of the data set and considering the results of the other studies cited above.

Attempts to calculate the fluxes of mass, heat, and salt through the BOMEX volume did not yield results which could be considered conclusive or consistent; therefore the results of these calculations are not presented.

5. CONCLUSIONS

Figure 11 shows that the general direction of the estimated current is northwest for Method 1 and southwest for Method 2. Either would seem to be a reasonable flow for this region of the ocean, but the former gives results slightly more in agreement with published representations of currents for the southwest North Atlantic Ocean. Defant (1964, p. 679) gives values of 3 to 9 cm s^{-1} to the northwest for the 800-m current east of Barbados. For determining geostrophic flow and property budgets in a large oceanic volume much better spatial resolution is required than what was available for this study. In the case of BOMEX, this would be about 30 nmi in the north-south direction, and somewhat longer in the east-west direction. The analysis presented here does, however, allow some insight into the net normal geostrophic flow between each pair of stations. But, in view of the very small values of current obtained by the use of either of the two methods as compared with the uncertainty between them, the problem of the applicability of the dynamic method to compute budgets for oceanic areas of much spatial variability when sampled at large horizontal intervals is still unresolved.

ACKNOWLEDGEMENTS

Funds for this analysis were provided by the National Science Foundation through its support of the International Decade for Ocean Exploration. I am indebted to Harris B. Stewart, Jr., Director, and Donald V. Hansen, Atlantic Oceanographic and Meteorological Laboratories of NOAA, for their kind support in the form of office space, staff assistance, computer time, and helpful criticisms. Joshua Z. Holland, Director, Eugene M. Rasmusson, and Vance A. Myers of NOAA's Center for Experiment Design and Data Analysis initially defined the problem and provided valuable suggestions and guidance. Christopher K.N. Mooers, Kamal Yacoub, and Claes Rooth of the University of Miami also contributed helpful comments. Paul A. Mazeika and Jon M. Hubertz of the Naval Oceanographic Office provided data for figures 9 and 10. Finally I am indebted to L.M. Fomin of the Institute of Oceanology, Moscow, for a helpful and spirited discussion of this analysis during his 1973 visit to NOAA's laboratories in Miami.

REFERENCES

- BOMAP Office, BOMEX Field Observations and Basic Data Inventory, National Oceanic and Atmospheric Administration, U.S. Department of Commerce, Rockville, Md., 1971, 428 pp.
- Defant, A., Physical Oceanography, Vol. I, MacMillan, New York, 1964, 729 pp.
- Delnore, V.E., "Diurnal Variation of Temperature and Energy Budgets for the Oceanic Mixed Layer During BOMEX," Journal of Physical Oceanography, Vol. 2, No. 3, 1972, pp. 239-247.
- Delnore, V.E., and J. McHugh, BOMEX Period III Upper Ocean Soundings, National Oceanic and Atmospheric Administration, U.S. Department of Commerce, Washington, D.C., 1972, 352 pp.
- Fomin, L.M., The Dynamic Method in Oceanography, Elsevier, Amsterdam, 1964, 212 pp.
- Holland, J.Z., "Preliminary Report on the BOMEX Sea-Air Interaction Program," Bulletin of the American Meteorological Society, Vol. 51, No. 9, 1970, pp. 809-820.
- Holland, J.Z., and E.M. Rasmusson, "Measurements of the Atmospheric Energy, Mass, and Momentum Budgets Over a 500-Kilometer Square of Tropical Ocean," Monthly Weather Review, Vol. 101, No. 1, 1973, pp. 44-55.
- Hubertz, J.M., "Long-Term Deep Current Measurements East of Barbados," Journal of Geophysical Research, Vol. 77, No. 21, 1972, pp. 3284-3286.
- Mazeika, P.A., "Circulation and Water Masses East of the Lesser Antilles," Deutsche Hydrografische Zeitschrift, Vol. 26, No. 2, 1973, pp. 49-73.
- Metcalf, W.G., "Shallow Currents Along the Northeastern Coast of South America," Journal of Marine Research, Vol. 26, No. 3, 1968, pp. 232-243.
- Neumann, G., and W.J. Pierson, Jr., Principles of Physical Oceanography, Prentice-Hall, Englewood Cliffs, 1966, 545 pp.
- Ryther, J.H., D.W. Mentzel, and N. Corwin, "Influence of the Amazon River Outflow on the Ecology of the Western Tropical Atlantic: I. Hydrography and Nutrient Chemistry," Journal of Marine Research, Vol. 25, No. 1, 1967, pp. 69-83.
- Scarlet, R., "Correlation Maps for the MODE-I Density Data," MODE Hot-Line News, No. 66, 1974, pp. 1-2.
- Sverdrup, H.U., M.W. Johnson, and R.H. Fleming, The Oceans, Prentice-Hall, New York, 1940, 1,087 pp.

Warsh, K.L., K.L. Echternacht, and M. Garstang, "Structure of Near-Surface Currents East of Barbados," Journal of Physical Oceanography, Vol.1, No. 2, April 1971, pp. 123-129.

Wüst, G., Stratification and Circulation in the Antillean-Caribbean Basins, Part I, Columbia University Press, New York, 1964, 201 pp.

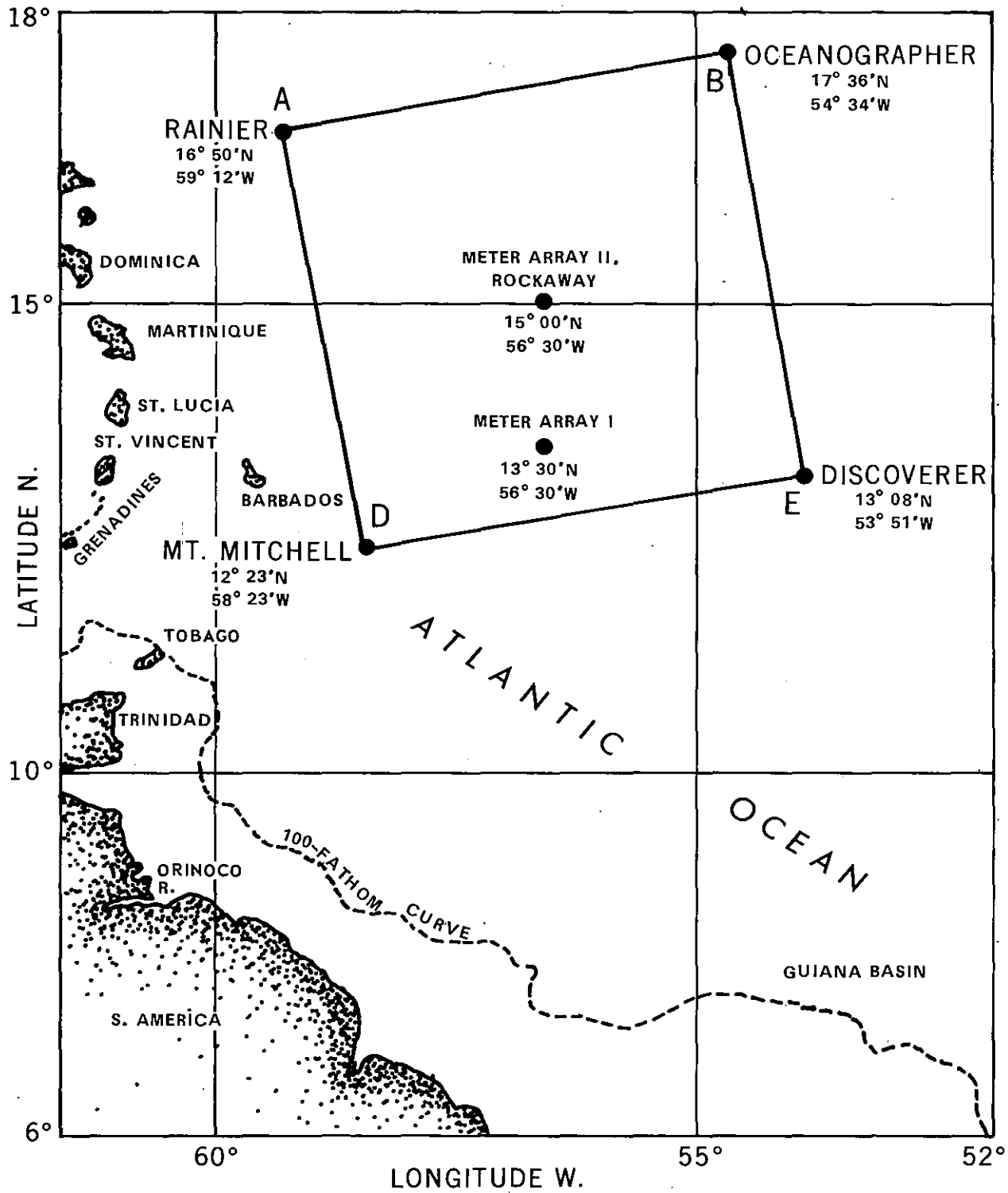


Figure 1.--The BOMEX array.

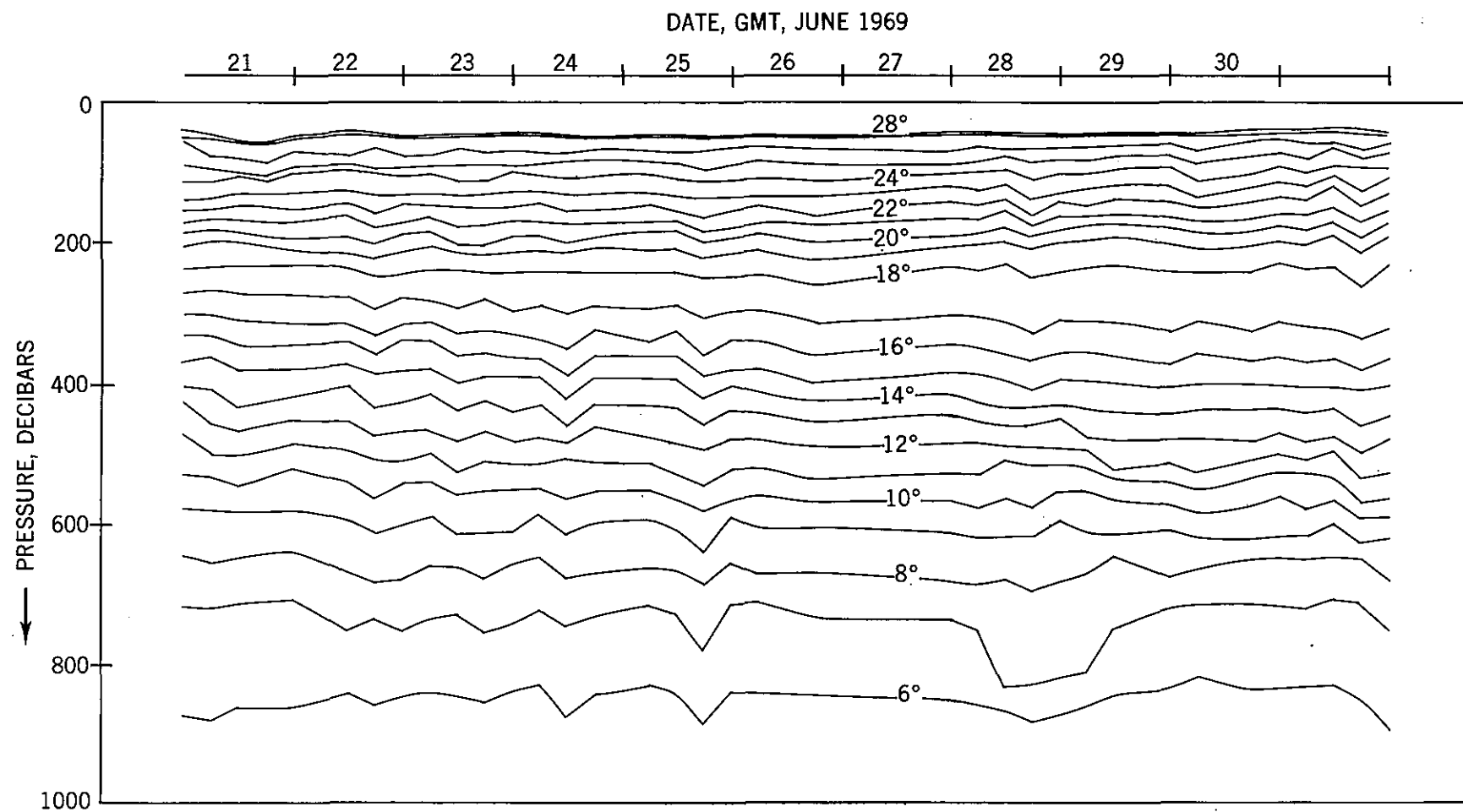


Figure 2.--Depths of isotherms, station A.

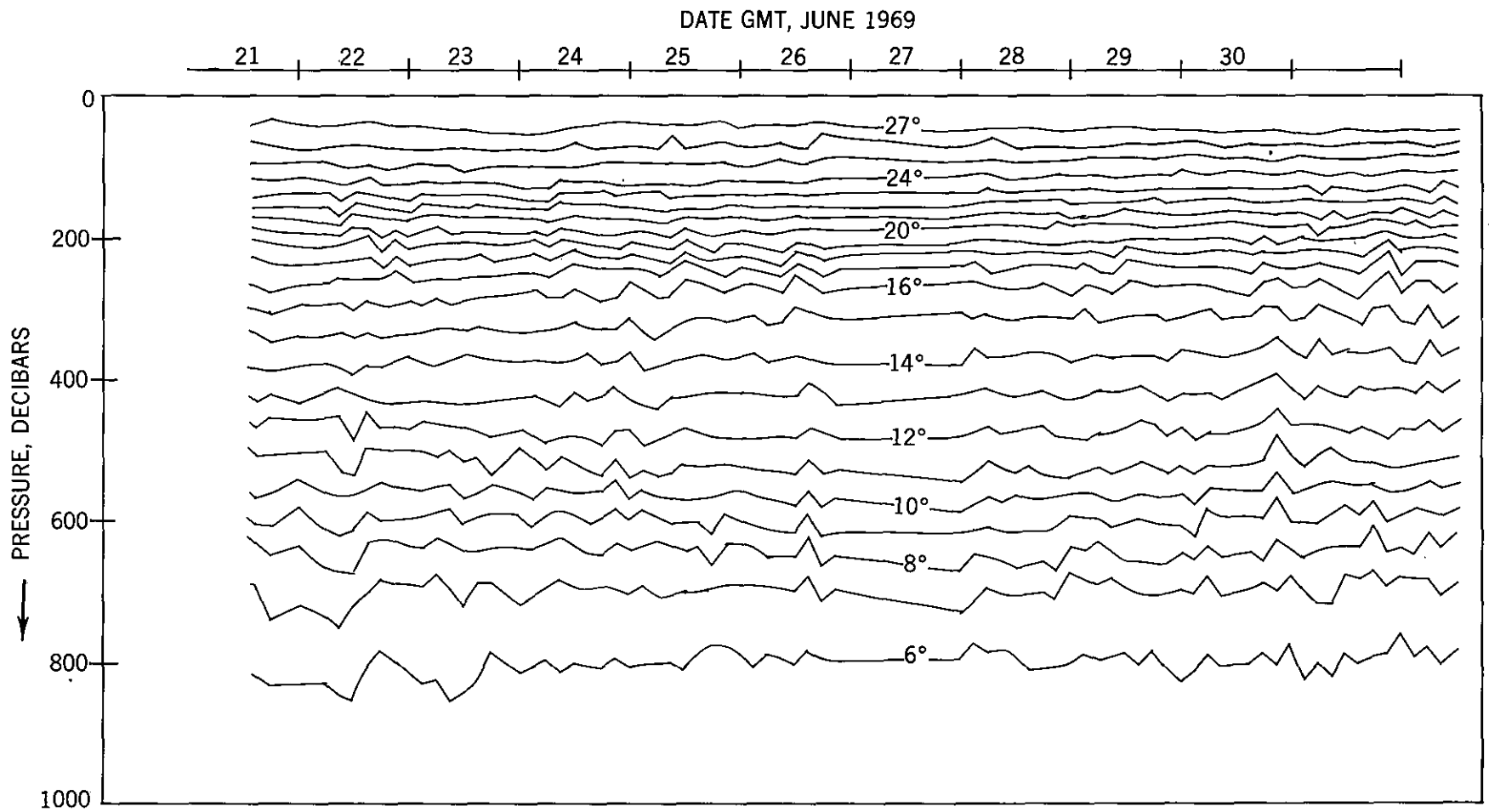


Figure 3.--Depths of isotherms, station B.

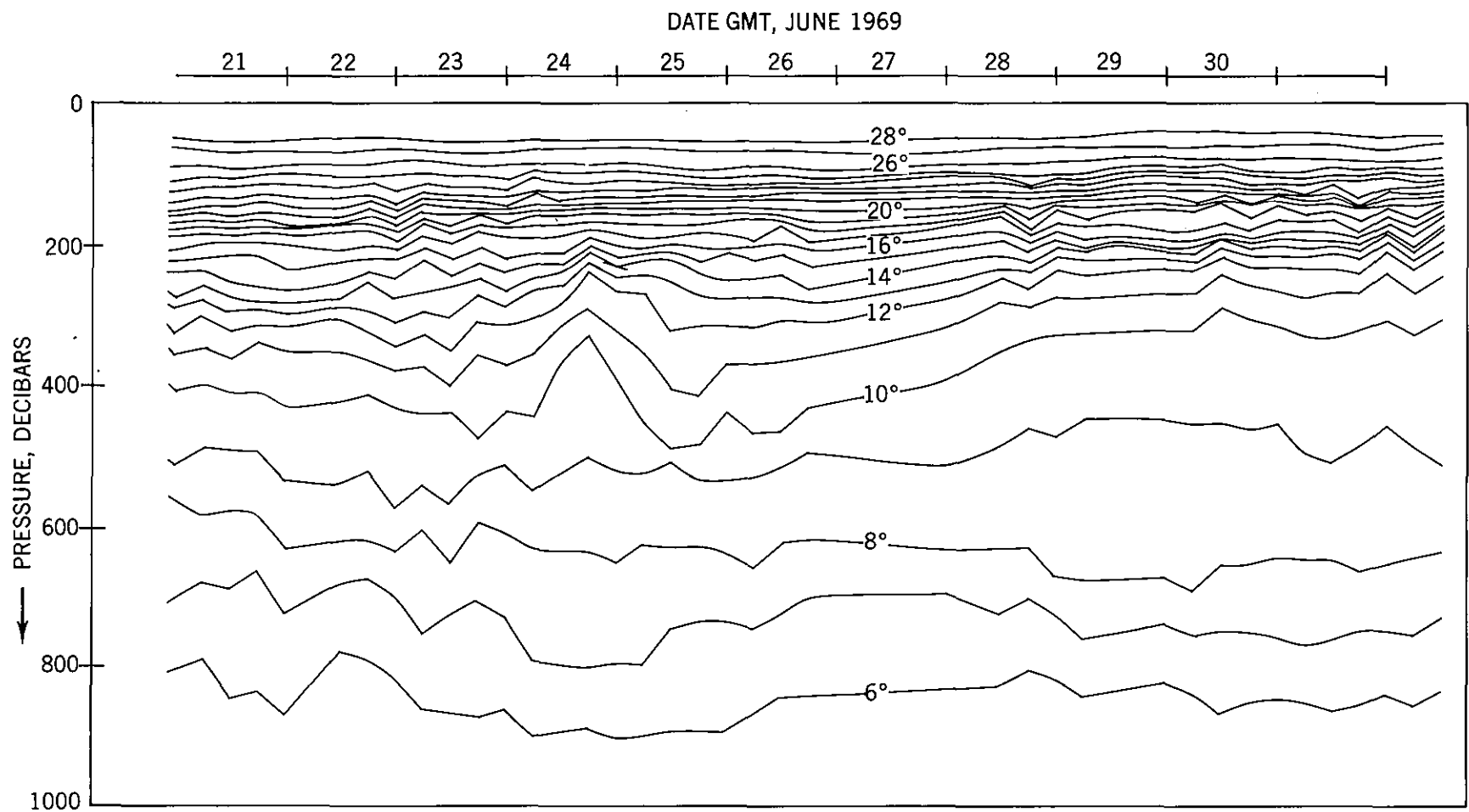


Figure 4.--Depths of isotherms, station D.

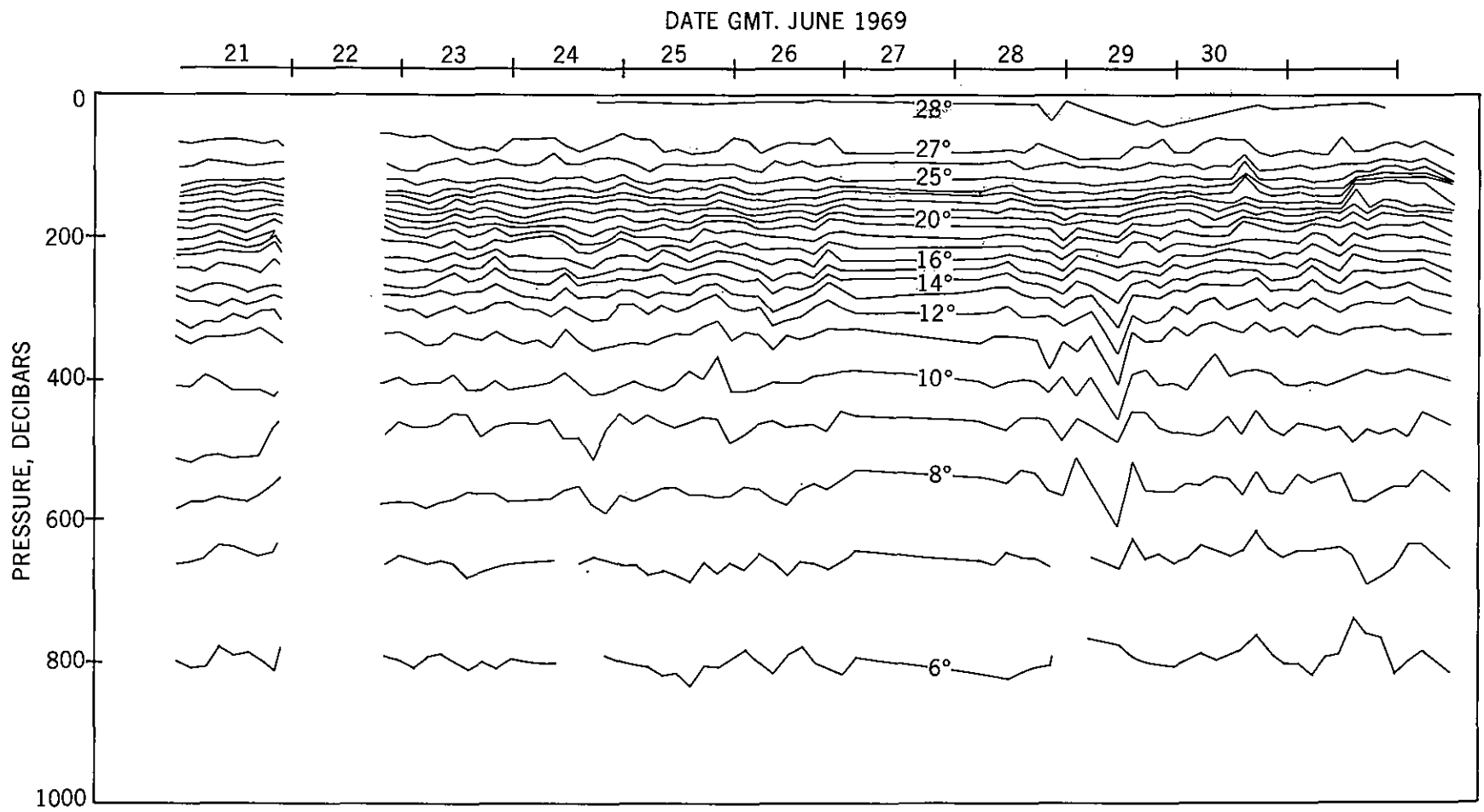


Figure 5.--Depths of isotherms, station E.

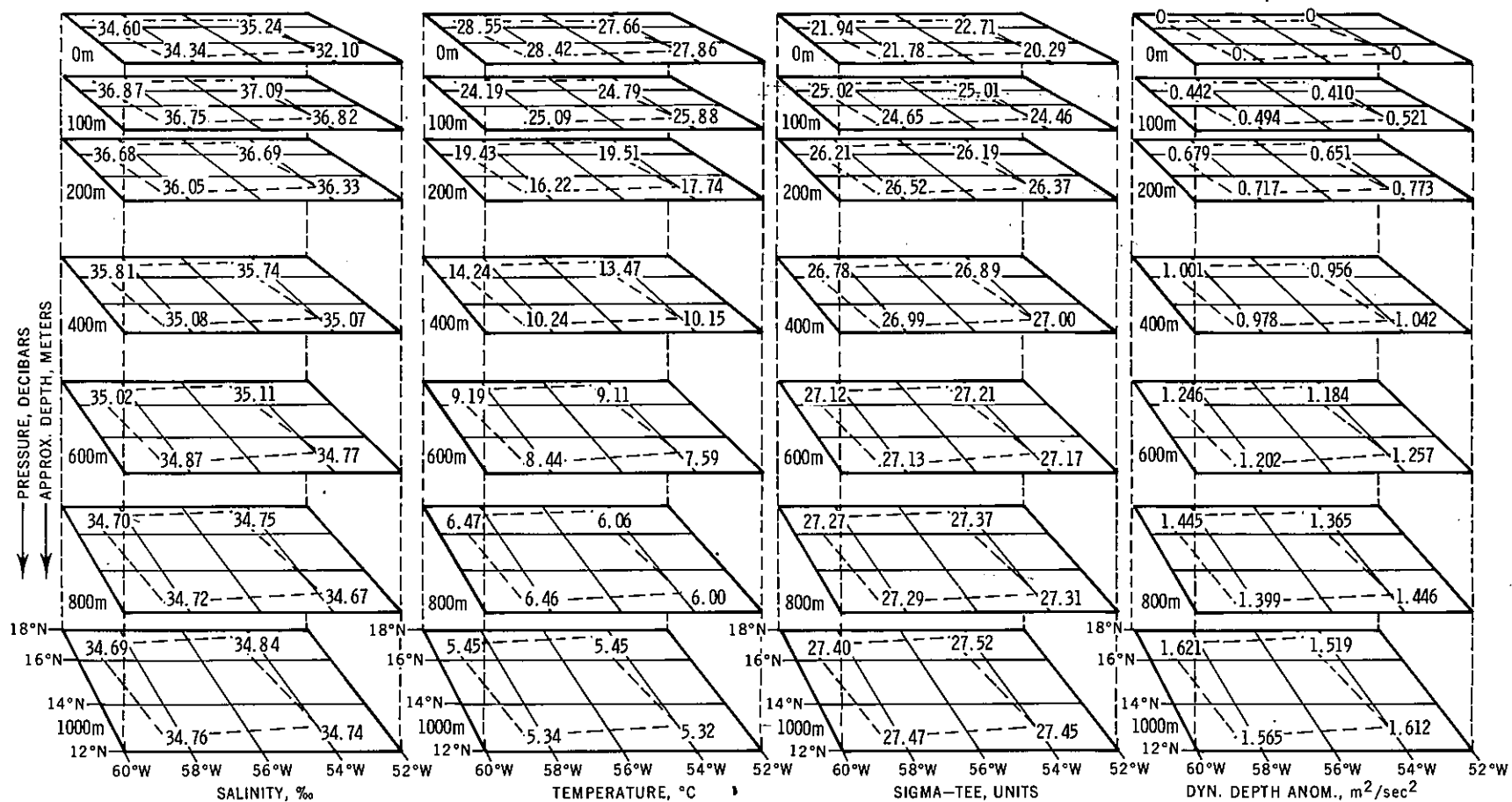


Figure 6.--Spatial variation of S , T , σ_t , and D .

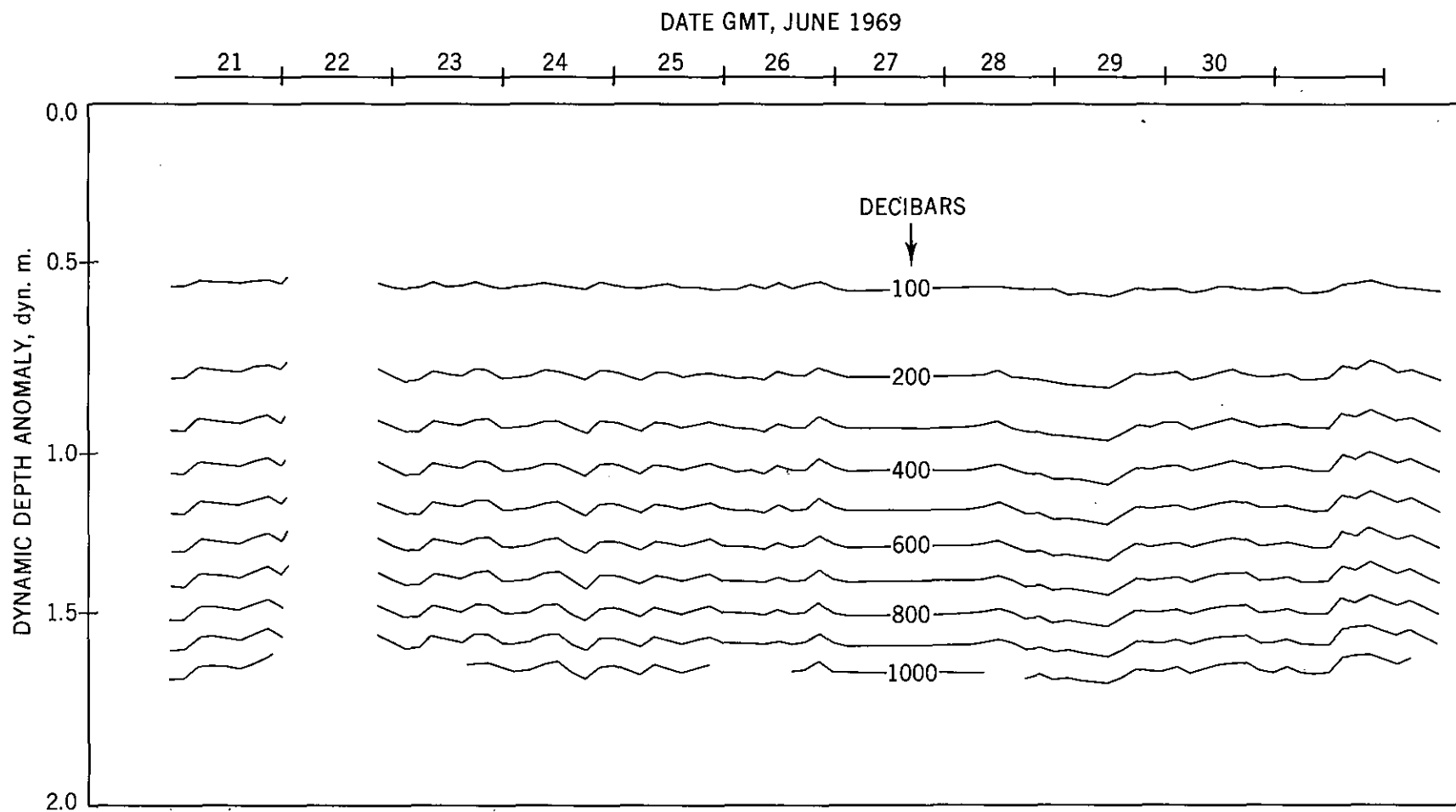


Figure 7.--Dynamic depth anomalies for certain isobars, station E.

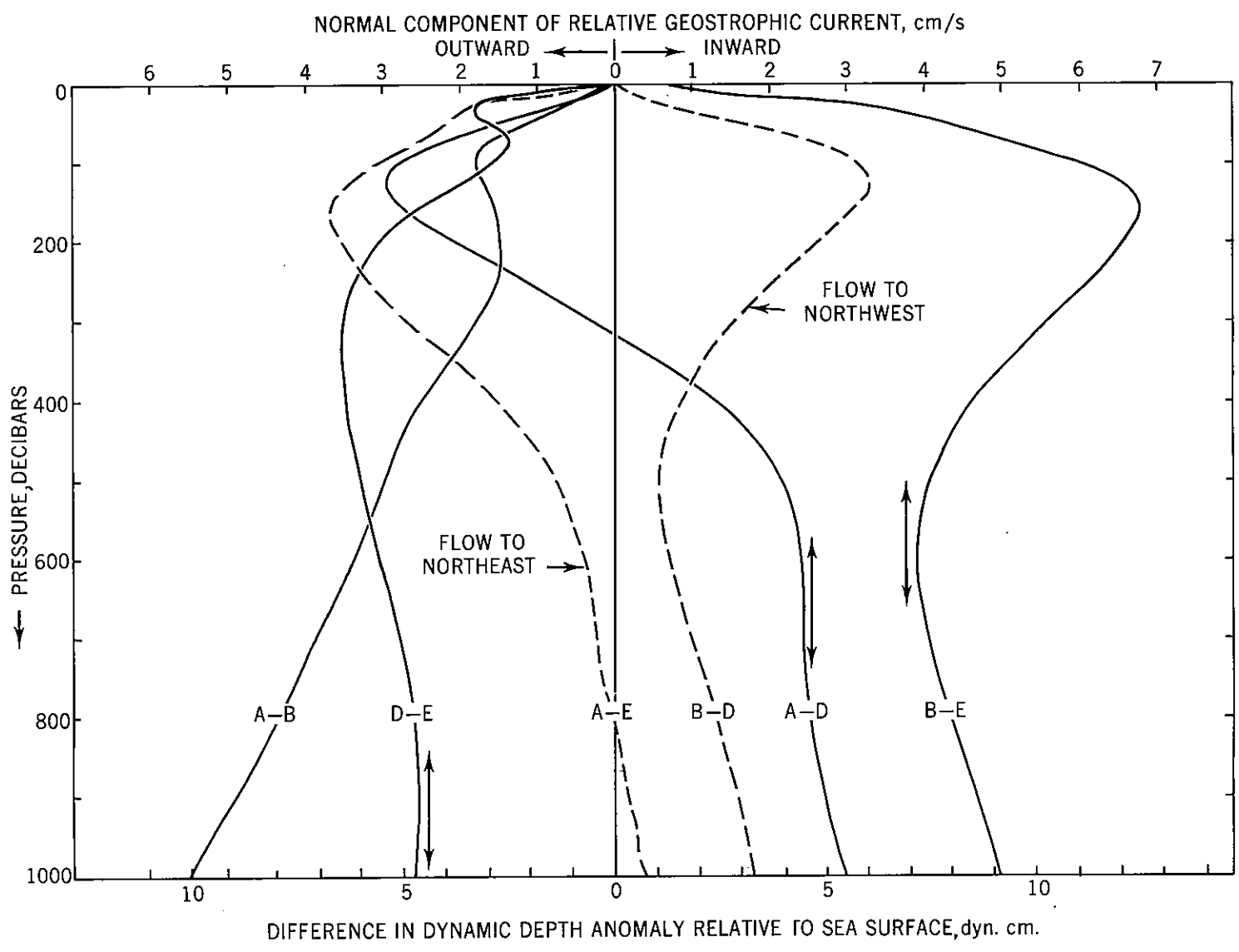


Figure 8.--Estimates of relative geostrophic profiles. (Lower scale does not apply to curves A-E and B-D.)

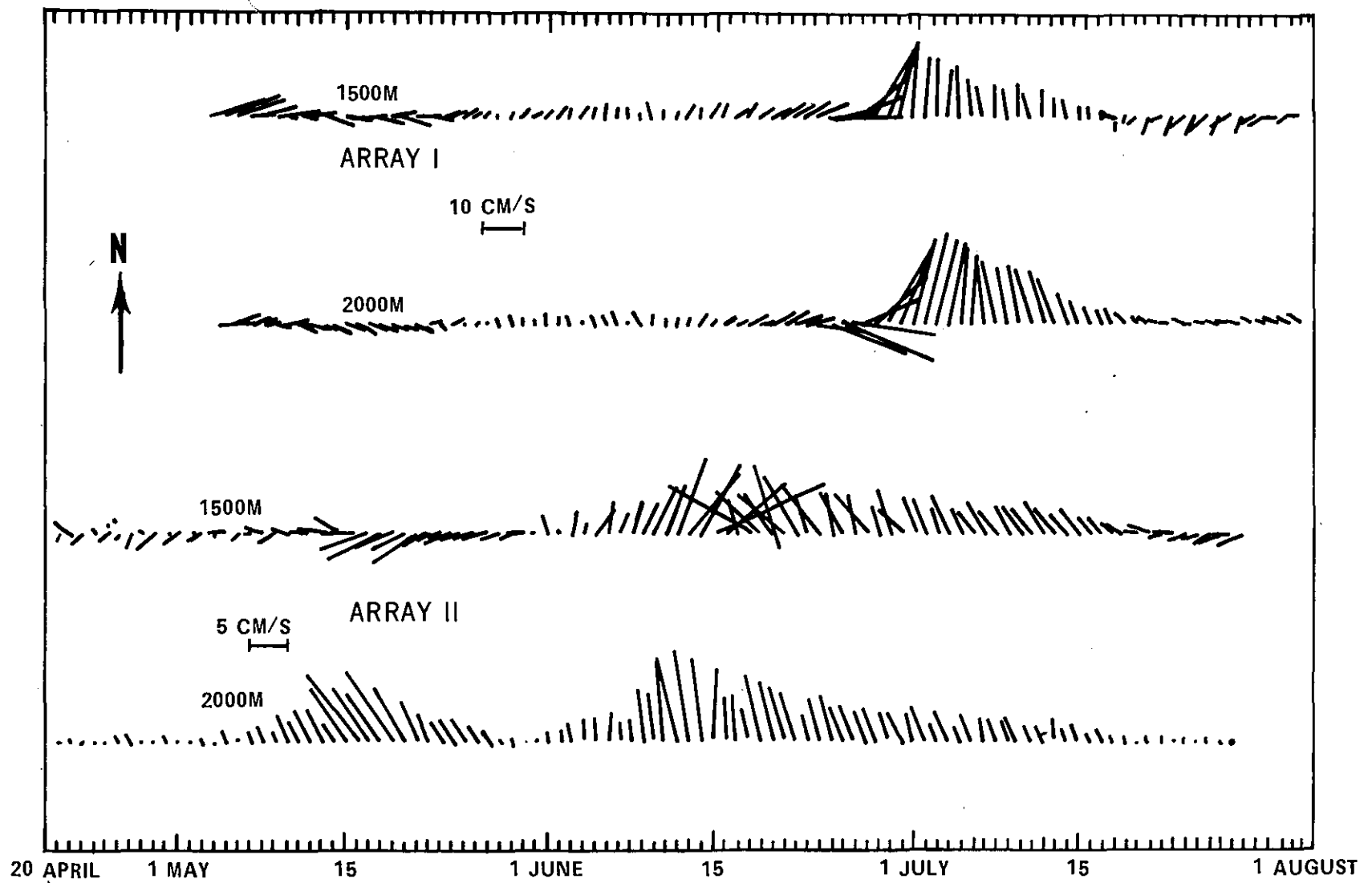


Figure 9.--Time histories of current meters at 1,500 and 2,000 m for arrays I and II.
 (Note change of scale between array I and array II.)

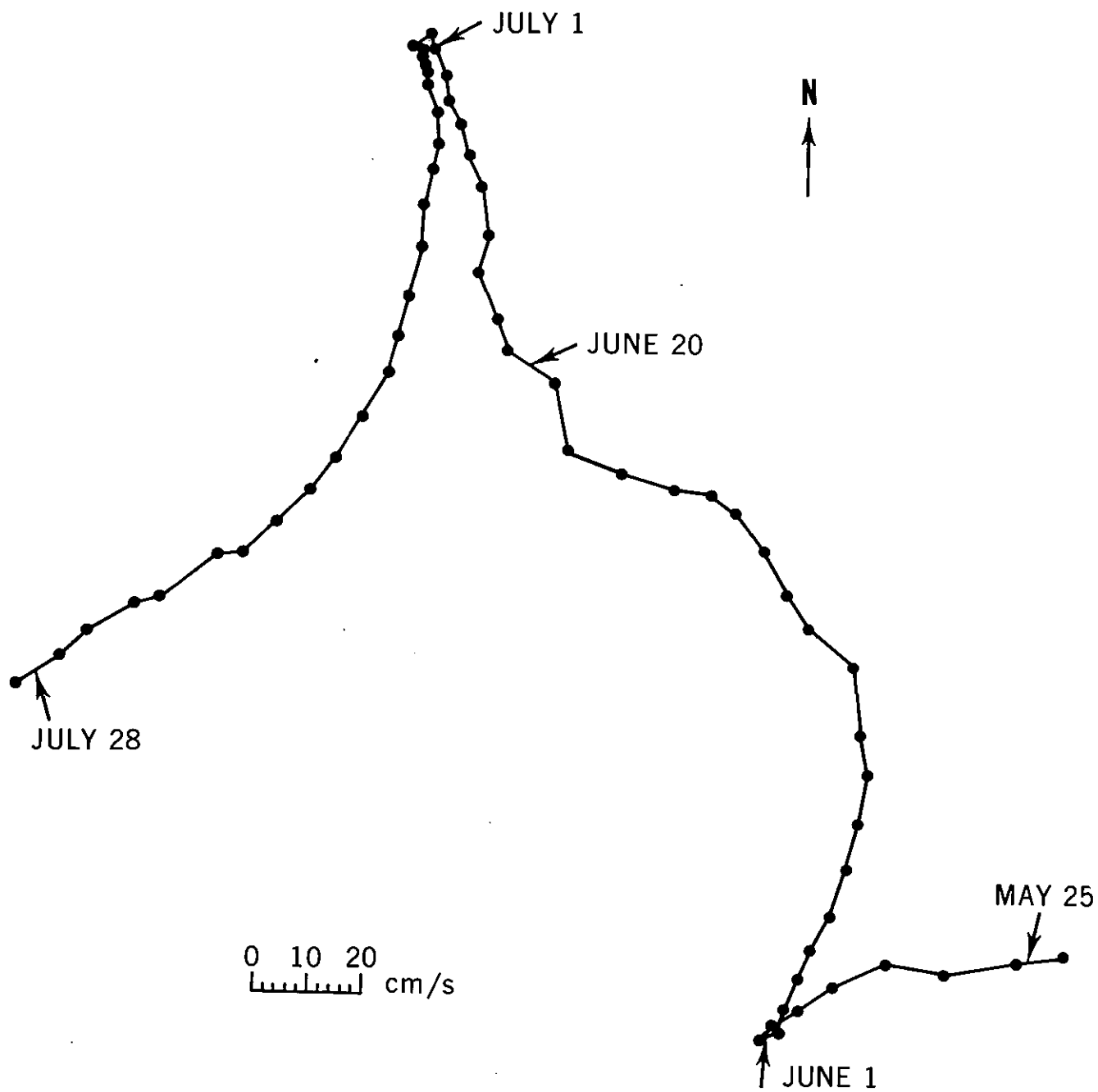


Figure 10.--Data from 300 m current meter.

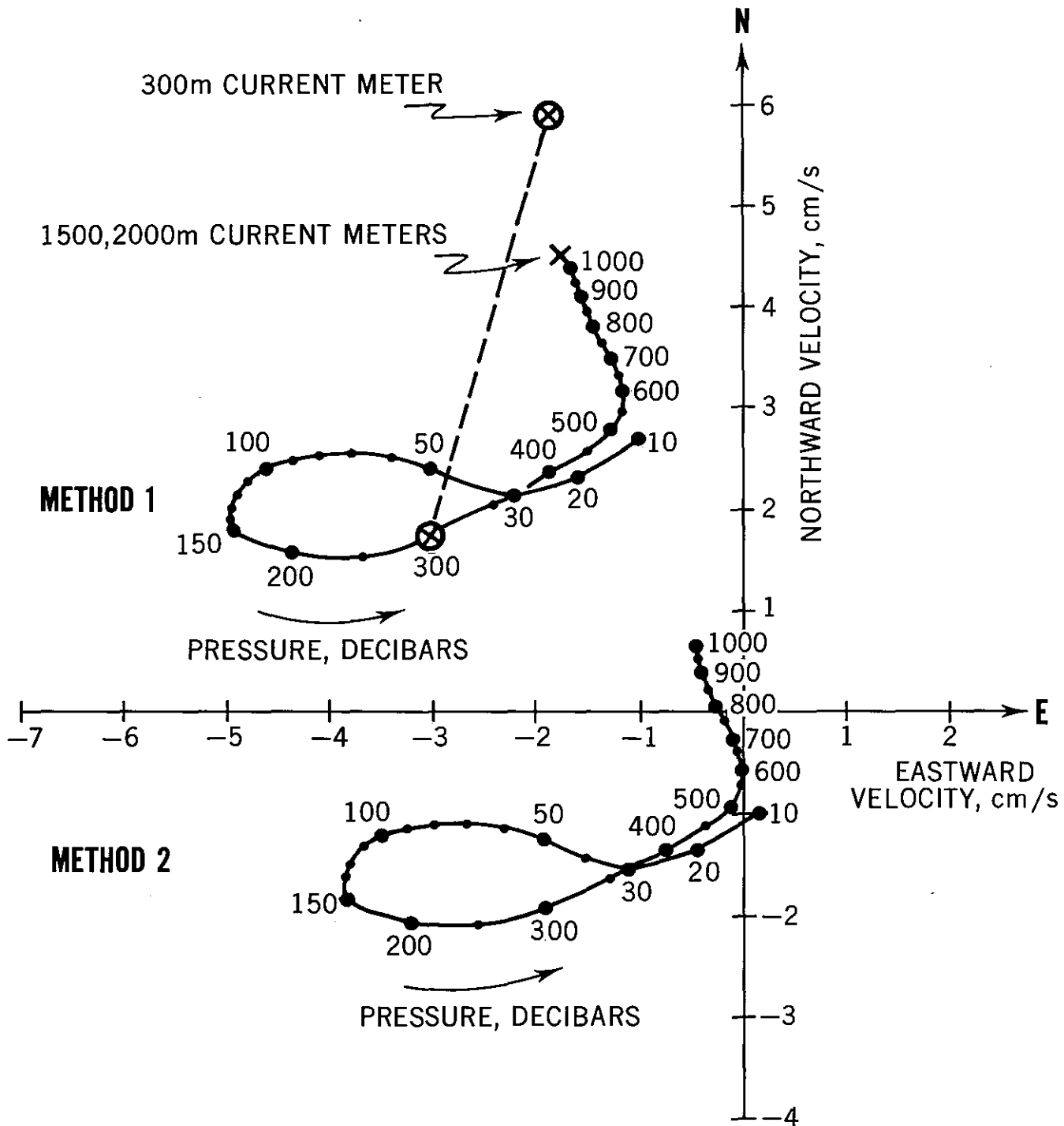


Figure 11.--Hodographs of interior motion.

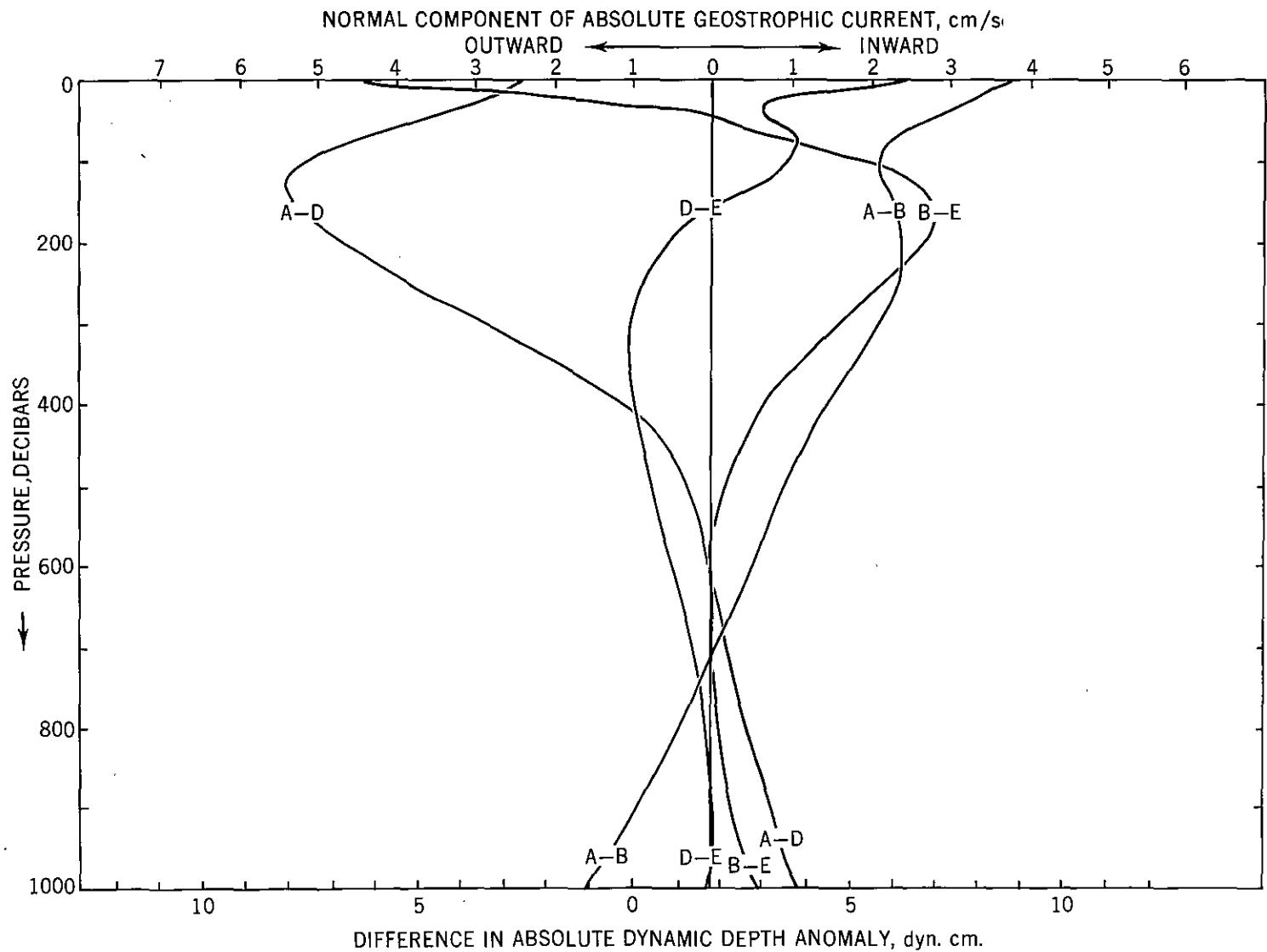


Figure 12.--Estimate of absolute geostrophic profiles.